# NATURAL PRODUCT COMMUNICATIONS

An International Journal for Communications and Reviews Covering all Aspects of Natural Products Research

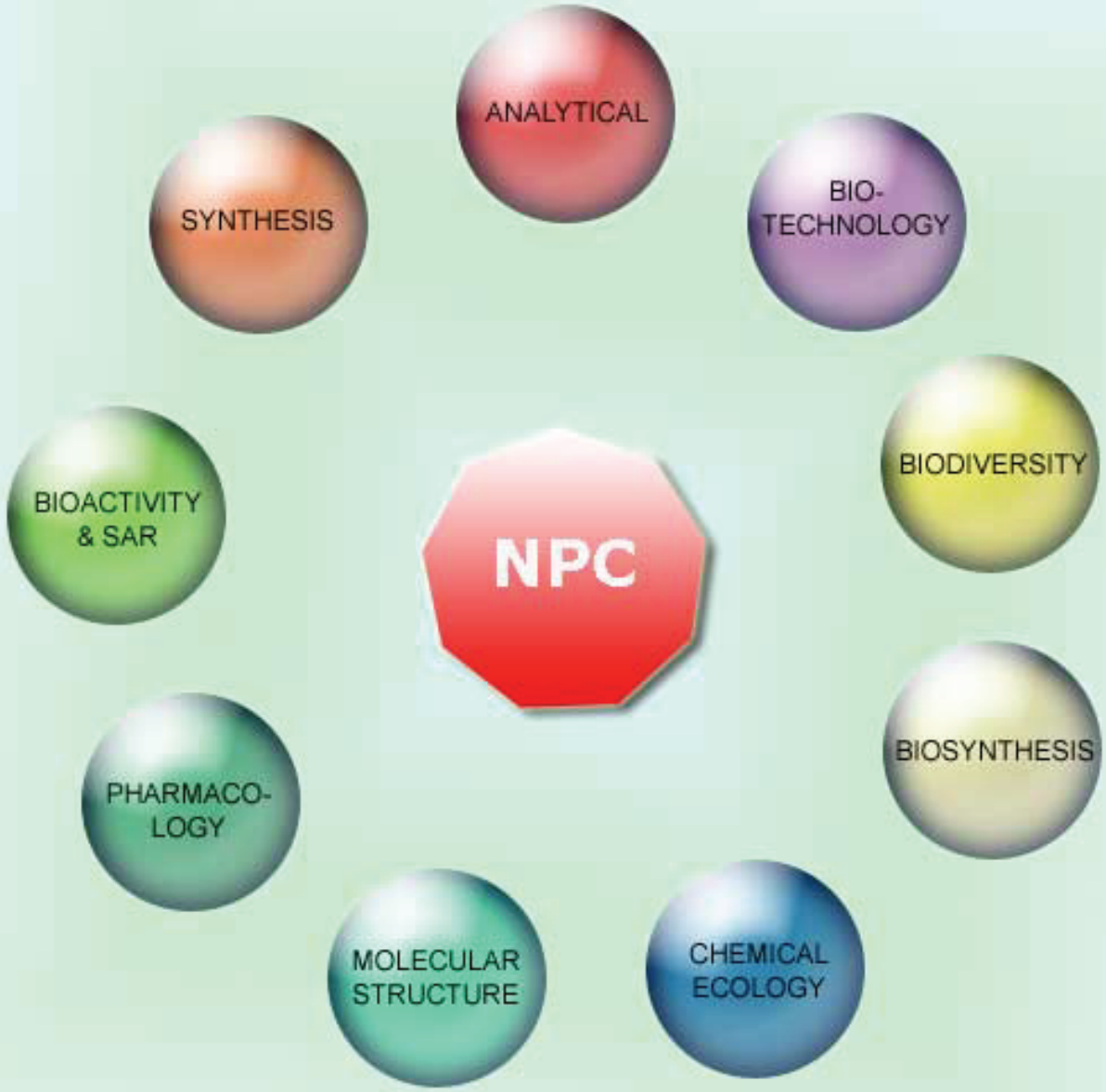


**This Issue is Dedicated to**
**Professor Dr. Mahabir P. Gupta**
**on the Occasion of his 75th Birthday**

Volume 14. Issue 1. Pages 1-160. 2019
ISSN 1934-578X (printed); ISSN 1555-9475 (online)
www.naturalproduct.us

# NPC Natural Product Communications




## INFORMATION FOR AUTHORS

Full details of how to submit a manuscript for publication in Natural Product Communications are given in Information for Authors on our Web site http://www.naturalproduct.us.




**To Subscribe**: Natural Product Communications is a journal published monthly. 2019 subscription price: US$2,595 (Print, ISSN# 1934-578X); US$2,595 (Web edition, ISSN# 1555-9475); US$2,995 (Print + single site online); US$595 (Personal online). Orders should be addressed to Subscription Department, Natural Product Communications, Natural Product Inc., 7963 Anderson Park Lane, Westerville, Ohio 43081, USA. Subscriptions are renewed on an annual basis. Claims for nonreceipt of issues will be honored if made within three months of publication of the issue. All issues are dispatched by airmail throughout the world, excluding the USA and Canada.

NPC Natural Product Communications

2019
Vol. 14
No. 1
1 - 4

# Synergism between Terbinafine and a *Neo*-clerodane Dimer or a Monomer Isolated from *Baccharis flabellata* against *Trichophyton rubrum*

**María Victoria Rodriguez[a], Estefanía Butassi[b], Matías Funes[c] and Susana A. Zacchino[b,*]**

[a]*Vegetal Biology Area*, *School of Biochemical and Pharmaceutical Sciences*, *National University of Rosario*, *2000- Rosario*, *Argentina*

[b]*Pharmacognosy Area*, *School of Biochemical and Pharmaceutical Sciences*, *National University of Rosario*, *2000- Rosario*, *Argentina*

[c]*INTEQUI-CONICET*, *Organic Chemistry Area*, *School of Chemistry*, *Biochemical and Pharmaceutical Sciences*, *National University of San Luis*, *5700- San Luis*, *Argentina*

*szaabgil@gmail.com*

**Received: September 5th, 2018; Accepted: December 25th, 2018**

The new *neo*-clerodane dimer (DACD) likely formed by a [4+2] photo-cycloaddition between two molecules of ent-15,16-epoxy-19-hydroxy-1,3,13(16),14-clerodatetraen-18-oic acid (DAC), both isolated from *Baccharis flabellata* Hook et Arn. var. *flabellata* (Asteraceae), were tested in combination with terbinafine (Terb) against *Trichophyton rubrum*. The interactions were assessed with different methodologies such as 3D *CombiTool* software, Loewe Combination Index (CI) and isobolograms. Results showed that the monomer DAC as well as its dimer DACD act synergistically with Terb against *T. rubrum*. DAC/Terb and DACD/Terb showed eight and twelve synergistic mixtures respectively in the *CombiTool* graphics thus suggesting that DACD/Terb was more synergistic with Terb than DAC. These results were corroborated by the CI values and the isobolograms of the detected combinations. DACD/Terb showed much lower CIs (0.34-0.47) than DAC/Terb (0.57-1.15) at the different inhibition percentages tested. Concomitantly, DACD/Terb isobolograms were more concave than for DAC/Terb at the different inhibition percentages. This is the first report showing antifungal synergistic interactions of *neo*-clerodanes dimers and add new evidences that *neo*-clerodanes monomers interact synergistically with Terb against *T. rubrum*.

**Keywords:** Terbinafine, *Trichophyton rubrum*, *Neo*-clerodane monomer, *Neo*-clerodane dimer, Synergism.

Diterpenoid dimers are a rather uncommon subclass of diterpenoids which are composed of two 20-carbon diterpenoid units linked through either one or two C-C bond, an ester bond or a ring moiety and are naturally synthesized mainly by an enzyme-catalyzed Diels Alder cycloaddition [1]. Among the great structural diversity of diterpenoid dimers, natural *neo*-clerodanes diterpene dimers have been scarcely reported up to date. A new dimer (DACD, Figure 1) was recently isolated by us from *B. flabellata* [2]. It showed to be formed *via* a [4+2] cycloaddition of *ent*-15,16-epoxy-19-hydroxy-1,3,13(16),14-clerodatetraen-18-oic acid (DAC) (Figure 1), one of the major *B. flabellata neo*-clerodanes. The structure elucidation and absolute configuration of DAC and DACD have been recently reported [2] and can be found as Supplementary data.

In another previous paper, we have reported that the *neo*-clerodanes monomers bacchotricuneatin A and bacrispine, isolated from *Baccharis tricuneata* (L.f.) Pers [3] and *Baccharis crispa* Spreng. respectively among other spp. [4,5] showed moderate antifungal activity against *Trichophyton rubrum* [6]. However, when tested in combination with terbinafine (Terb), their activities were highly enhanced. Considering this previous finding, the antifungal activity of the clerodane dimer DACD as well as its monomer DAC were tested here alone and in combination with Terb against *T. rubrum* in order to have a look on the anti-*T. rubrum* enhancing behavior of a *neo*-clerodane dimer in comparison with the monomer.

*T. rubrum* is the major dermatophyte that cause human skin, nail and eye infections [7] and although superficial fungal infections are not life threatening, they usually are very difficult to eradicate and new antifungal compounds are highly needed.

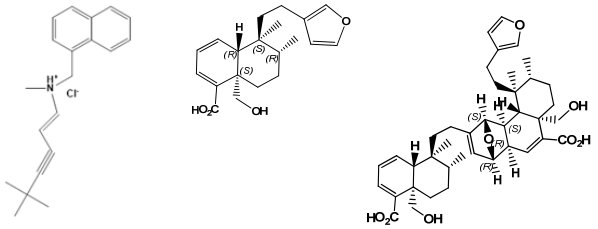

**Figure 1:** Structures of terbinafine (left), DAC (medium) and DACD (right)

Regarding the selected antifungal drug, it is well-known that Terb (Figure 1) is the preferred antifungal drug to treat superficial mycoses produced by dermatophytes [8] although it shows various side-effects that include liver problems and allergic reactions.

Considering that the combination of a single natural product with an antifungal chemosynthetic drug can improve the effectiveness of the antifungal drug at a lower dose [9], combination of Terb/DAC or Terb/DACD could take advantage of the high activity of Terb highly diminishing its side effects and also preventing or delaying the emergence of resistant populations of the pathogenic fungus.

Regarding the several methods of choice to test compounds in combination [10,11], we first selected a three-dimensional (3D) study with the *CombiTool* software [12]. The 3D-model is considered the most complete way to identify the regions of significant synergy and antagonism, and presents a complete map of drug interactions in a way that can be easily interpreted.

*CombiTool* software first needs the construction of single-agent dose-response curves for the calculation of zero interaction response surfaces [12]. The parameters 'a' and 'm' obtained from these curves are used by the software to generate a 3D-zero interaction surface (represented in green in Figure 2), according to the Loewe additivity criteria.

Then, the experimental effects of DAC/Terb (A) and DACD/Terb (B) combinations (formed with different ratios of each partner) were introduced in *CombiTool* software. Any statistically significant deviation of these combinations from the zero interaction surface is indicated by the position of red balls, each representing one combination (Figure 2). Balls over the zero interaction surface are indicative of synergism; within the surface, are indicate of additivism and below the surface, of antagonism. The red balls in Figure 2 for DAC/Terb and DACD/Terb show the interactions at all effect levels (from 1 to 100 % inhibition). However, for the sake of clarity, only the synergistic combinations with > 50 % inhibition level are represented in Figure 2.

Figure 2 shows that eight combinations of DAC/Terb and twelve combinations of DACD/Terb showed synergism, thus suggesting that not only the monomer DAC but its dimer DACD interact synergistically with Terb, although DACD show more synergistic combinations with an inhibition effect ≥ 50 %. In Table 1, the composition of the combinations and the percentages of inhibition at which they showed synergism are detailed.

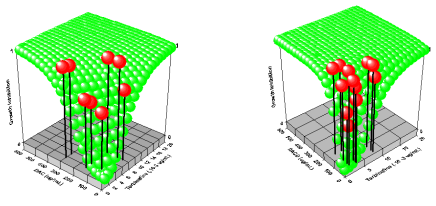

**Figure 2:** Surfaces of experimental effects for DAC/Terb (left), DACD/Terb (right) obtained with *CombiTool* software. Red spheres over the surface correspond to combinations that show synergism with an inhibition effect ≥ 50 %.

In a second step, the CI of the synergistic combinations detected with the *CombiTool* software were calculated as follows: an inoculum of *T. rubrum* was incubated with serial dilutions of Terb (7.8, 3.9 and 1.56 x $10^{-3}$ µg/mL), added with fixed sub-inhibitory concentrations of DAC (300, 150, 75, 37.5, 18.75 or 9.38 µg/mL) or DACD (150, 75, 37.5, 18.75 or 9.38 µg/mL). The % of growth for Terb and each combination were represented in dose-response curves (Figure 3). In the two-drug combinations curves of Terb added with different fixed concentrations of DAC (Figure 3A) or DACD (Figure 3B), it is clear that both *neo*-clerodanes decreased the $MIC_{50}$, $MIC_{70}$, $MIC_{90,}$ and $MIC_{100}$ (dotted lines a-d) of Terb, thus enhancing its antifungal capacity with lower doses. The $MIC_{50}$, $MIC_{70}$, $MIC_{90,}$ and $MIC_{100}$ values of Terb, DAC and DADC alone and in dual combinations DAC/Terb and DACD/terb along with the Dose Reduction Index (DRI) and the CI are shown in Table 2.

**Table 1:** Synergistic combinations of DAC/Terb and DACD/Terb detected with the *CombiTool* software. The number between each bracket indicates the percentage of inhibition at which each combination showed synergism (S).

| | Conc. µg/mL | | | | | | | | | | | |
|---|---|---|---|---|---|---|---|---|---|---|---|---|
| | 300 | | 150 | | 75 | | 37.5 | | 18.75 | | 9.38 | |
| Terb | DAC | DACD | DAC | DACD | DAC | DACD | DAC | DACD | DAC | DACD | DAC | DACD |
| 7.80x $10^{-3}$ | - | - | S (100) | | S (100) | S (100) | S (70) | S (100) | - | S (90) | - | - |
| 3.12x $10^{-3}$ | S (90) | - | S (70) | S (100) | S (70) | S (100) | - | S (90) | - | S (90) | - | S (70) |
| 1.56x $10^{-3}$ | S (90) | - | S (70) | S (100) | - | S (90) | - | S (50) | - | S (50) | - | - |

**Table 2:** Antifungal activity of terbinafine (Terb) and the *neo*-clerodane monomer (DAC) and dimer (DACD) at different inhibition percentages ($MIC_{100}$, $MIC_{90}$, $MIC_{70}$ and $MIC_{50}$) either alone or in the two-drug combinations DAC/Terb and DACD/Terb. The Combination Index (CI) and the Dose-Reduction Index (DRI) in combination were calculated for *Trichophyton rubrum* fungal sp.

| | MICs in µg/mL | | | | | | |
|---|---|---|---|---|---|---|---|
| | MICs at different inhibition % | $MIC_{DAC}$ alone | $MIC_{Terb}$ alone x$10^{-3}$ | $MIC_{DAC}$ in comb | $MIC_{Terb}$ in comb x$10^{-3}$ | CI | DRI Terb |
| DAC/ Terb | $MIC_{100}$ | 558.0 ± 10.2 | 15.6 ± 1.1 | 75.0 ± 1.1 | 7.8 ± 0.6 | 0.6 | 2.0 |
| | $MIC_{90}$ | 409.0 ± 7.9 | 14.4 ± 0.8 | 300.0 ± 0.1 | 3.1 ± 0.0 | 0.8 | 4.6 |
| | $MIC_{70}$ | 312.0 ± 5.3 | 9.4 ± 0.2 | 75.0 ± 0.9 | 3.1 ± 0.1 | 0.6 | 3.0 |
| | $MIC_{50}$ | 258.0 ± 6.3 | 7.2 ± 0.0 | 18.5 ± 0.8 | 7.8 ± 0.1 | 1.2 | 0.9 |
| | | $MIC_{DACD}$ alone | | $MIC_{DACD}$ in comb | | | |
| DACD/ Terb | $MIC_{100}$ | 274.0 ± 3.5 | 15.6 ± 1.4 | 75.0 ± 3.8 | 3.1 ± 0.5 | 0.5 | 5.0 |
| | $MIC_{90}$ | 145.0 ± 2.4 | 14.4 ± 0.8 | 18.8 ± 1.5 | 3.1 ± 0.1 | 0.3 | 4.6 |
| | $MIC_{70}$ | 99.0 ± 4.2 | 9.4 ± 0.8 | 9.4 ± 2.3 | 3.1 ± 0.1 | 0.4 | 3.0 |
| | $MIC_{50}$ | 77.0 ± 3.1 | 7.2 ± 0.0 | 18.8 ± 1.1 | 1.6 ± 0.0 | 0.5 | 4.6 |

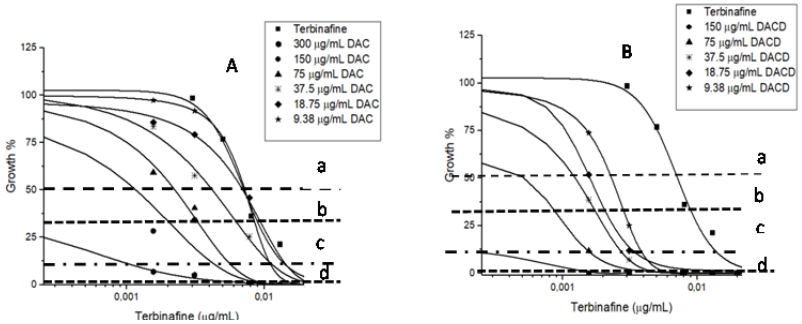


**Figure 3:** Dose-response curves of terbinafine with fixed concentrations of the monomer DAC (A) and the dimer DACD (B) against *Trichophyton rubrum*. The response is presented as percentage of growth. The horizontal dotted lines at 50 % inhibition (50% growth) (a); 70 % inhibition (30 % growth) (b); 90 % inhibition (10 % growth) (c) and 100 % inhibition (0 % growth) (d) were drawn for an easier comparison of DAC's and DACD's effects against *T. rubrum*.

From Table 2 it is clear that DACD/Terb is more synergistic than DAC/Terb since DACD/Terb showed much lower CIs (0.3-0.5) than DAC/Terb (0.6-1.2), being the ratio DACD (18.75 µg/mL)/Terb (3.12 x $10^{-3}$ µg/mL) the one that showed the most synergistic interaction for displaying a percentage of inhibition of 90 %. For achieving a 100 % inhibition, the ratio should be 75 µg/mL DACD/3.12 x $10^{-3}$ µg/mL Terb. In this combination the $MIC_{100}$ of Terb decreased 5-fold (from 15.60 to 3.12 x $10^{-3}$ µg/mL, DRI = 5) and the $MIC_{90}$, from 14.37 to 3.12 x $10^{-3}$ µg/mL with DRI = 4.6. In contrast, the $MIC_{100}$ and $MIC_{90}$ of Terb decreased 2- and 4.6-fold (DRI = 2.0 and 4.6) when combined with DAC showing lower synergistic interaction with CIs = 0.6 and 0.8 respectively.

For combinations that produced 70 or 50 % inhibition, also DACD showed better interaction effects (CIs = 0.4-0.5, with DRIs = 3.0 and 4.6) than DAC (CI = 1.2-0.6, with DRIs= 3.0-0.9). The corresponding isobolograms show the behavior of the combinations at the different effect levels [13]. The isobolograms at 100 % inhibition are presented in Figure 4. They are representative of the isobolograms at other effect levels such as 50, 70 and 90 % inhibition percentages.

The comparison of the isobologram of DACD/Terb (left) with that of DAC/Terb (right) at the same effect level shows that the isobologram of DACD/Terb have higher concavity than that of DAC/Terb, corroborating that DACD showed a greater synergism with Terb than DAC.

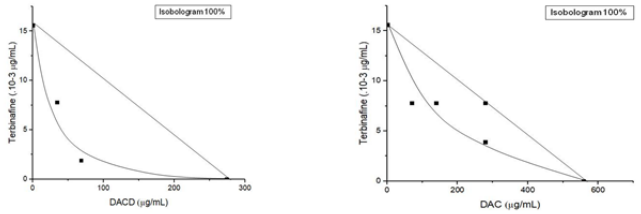


**Figure 4:** Isobolograms of the combinations DACD/Terb (left) and DAC/Terb (right) at 100 % effect level. $MIC_{100}$ of Terb is plotted in the *y*-axis and of DACD or DAC on the *x*-axis. The lines connecting the MIC in each isobologram of each partner is the line of additivity. Points located below the line indicate synergy, above the line antagonism and on the line additivity.

As conclusions, we could demonstrate that the *neo*-clerodane monomer DAC as well its dimer DACD behave synergistically with Terb against *T. rubrum*. However, the dimer DACD showed a higher synergism than DAC clearly demonstrated by different methodologies such as 3D, CI and isobolograms.

Regarding the monomer DAC, the results of this work add new evidences that the monomers of *neo*-clerodanes interacts synergistically with Terb against *T. rubrum*. As for the dimer DACD, this is the first report on the synergism of a *neo*-clerodane dimer with Terb against *T. rubrum* and also the first demonstration that it is a better enhancer of the activity of the antifungal drug Terb. Both compounds, mainly the dimer, enhance the activity of Terb at lower doses than the required for acting alone. Since Terb produces unwanted side effects, the fact that it can be used in combination at lower amounts with the same effectivity, is an important finding for a future pharmaceutical development of these combinations.

## Experimental

***Chemicals:*** Terb hydrochloride (≥ 98%) was purchased from Sigma-Aldrich (St Louis, MO, USA). DAC and DACD (≥ 98% each) were isolated from of *B. flabellata* as reported in [2]. Their HPLC profiles are shown in Supplementary Material Figures 1S and 2S. One specimen of *B. flabellata* was deposited in the Herbarium of the National University of San Luis (UNSL voucher number L.A. Del Vitto & E.M. Petenatti # 9436).

***Fungal strain and inoculum preparation:*** *T. rubrum* CCC 110 (CEREMIC, Centro de Referencia en Micología, Facultad de Ciencias Bioquímicas y Farmacéuticas, Rosario, Argentina) was used for the antifungal evaluation. This is the same strain used in the previous paper [6]. The growth of the strain was performed on Sabouraud-chloramphenicol agar during 7 d at 30°C, maintained on slopes of Sabouraud-dextrose agar (SDA) (Oxoid, Ontario, Canada). Inocula were adjusted to 1-5 × 103 spores with colony forming units (CFU)/mL [14].

***Determination of MIC:*** Minimum Inhibitory Concentration (MIC) was determined according to the guidelines of the CLSI for filamentous fungi (M38 A2) [14]. Dilutions of stock Terb or pure compounds in DMSO (final concentration ≤1%) in RPMI-1640 (Sigma-Aldrich) (200 µL) were poured into the first well of a 96-well microplate, and then, 100 µL were transferred to the next well containing 100 µL of RPMI-1640 buffered to pH 7.0 with 4-morpholinepropanesulfonic acid (MOPS, Sigma-Aldrich). A volume of 100 µL of inoculum suspension was added to each well (for sterility control, sterile water was added to the well instead) rendering concentrations from 1-30 x $10^{-3}$ µg/mL for Terb and from 800 to 31.25 µg/mL for pure compounds. Plates were incubated for 7 days at 28-30°C in a moist, dark chamber. $MIC_{100}$ was defined as the lowest concentration of Terb or pure compound resulting in total inhibition of visual growth compared to the growth in the control wells containing no antifungal. Tests were carried out in duplicate.

***Determination of growth inhibition percentages of T. rubrum and $MIC_{50}$, $MIC_{70}$, $MIC_{90}$ of DAC and DACD:*** *T. rubrum* growth inhibition was obtained by image analysis **[6,15]**. After incubation, the plates with the assays were placed on an Epichemi3 darkroom (UVP, Upland, CA, USA). Photographs of each plate were recorded with a high resolution cooled digital monochrome CCD camera (Hamamatsu C8484-51-03G). Pictures were analyzed using LabWorks version 4.6 (UVP) MacBiophotonics ImageJ and according to the steps previously described [6].

***Analysis with CombiTool software:*** Eighteen combinations of Terb and each pure compound (DAC or DACD) were tested. Sub-inhibitory concentrations for DAC ($MIC_{100}$ = 558.95 µg/mL) and DACD ($MIC_{100}$ = 274.84 µg/mL) and 1/2, 1/5 and 1/10 MIC for Terb ($MIC_{100}$ = 15.6 × $10^{-3}$ µg/mL) were combined in a microtiter tray by duplicate as described for $MIC_{100}$ determinations above. The inhibition percentage of each combination was determined after 7 days incubation time by image analysis. The program used to obtain graphs was the *CombiTool* kindly provided by Dr. Jürgen Sühnel (Jena, Germany) [12]. Dose-responses curves for DAC, DACD and Terb were performed and parameters "a" and "m" were determined by the median-effect equation [16] with the nonlinear regression module of the Origin software package (www.originlab.de). Loewe Additivity response surface (LA) was calculated for DAC, DACD and Terb with a and m parameters. The comparison of the surface obtained with experimental data *vs* the zero response surface allows the direct visualization of spheres which, if they fall into the surface are indicative of additivism, over the surface indicate synergism and below the surface show antagonism.

***Analysis of the combination effect:*** The nature of the interaction (synergy, additivity, or antagonism) between an individual DAC or DACD and Terb as a function of their concentrations and fungal

growth inhibition ($MIC_{50}$, $MIC_{70}$, $MIC_{90}$, $MIC_{100}$) was assessed by the combination index (CI) [16] as follows:

$$CI = \frac{MIC_x \text{ Terb in comb}}{MIC_x \text{ Terb alone}} + \frac{MIC_x \text{ NC}^* \text{ in comb}}{MIC_x \text{ NC}^* \text{ alone}}$$

Where x refers to the inhibition percentage and can be 50, 70, 90 or 100 %; * NC represents one of the natural neo-clerodanes that can be DAC or DACD.

CI helps to identify synergistic (CI < 1), additive (CI = 1), and antagonistic interactions (CI > 1) [16].

The dose reduction index (DRI) is a measure of how many -fold the concentrations in the combination may be reduced as compared with the doses of each drug alone [16] and is calculated as follows:

$$DRI = \frac{MIC_x \text{ of Terb alone}}{MIC_x \text{ Terb in combination}}$$

DRI > 1 is beneficial, indicating synergism and is important in clinical situations, in which dose reduction leads to reduced toxicity while the therapeutic efficacy is retained [16].

***Isobolograms:*** The isobologram illustrates the result of the checkerboard assay and the CI values. The axis of the isobologram represents the dose of DAC or DACD and the ordinate represents the dose of Terb. The straight line connecting the MIC points represents zero interaction [13]. Below and above this line the areas of synergistic and antagonistic interactions respectively are found. The concentrations of the two drugs used in combination to provide the same effect (50, 70, 90 or 100 % inhibition) were placed in the same plot.

**Supplementary data:** Median-effect equation parameters of pure compounds Terb, DAC and DACD and UV-Vis spectrum, HPLC-DAD of DAC and DACDs and isobolograms at all effect levels are available in electronic form on the publisher's website.

**Acknowledgments -** This research was supported by *Agencia Nacional de Promoción Científica y Tecnológica* (ANPCyT), PICT2014-117. EB and MVR acknowledge *Consejo Nacional de Investigaciones Científicas y Técnicas* (CONICET) and are members of the teaching staff of Biochemical and Pharmaceutical Sciences School, National University of Rosario, Argentina. MF would like also thank especially to the research projects: PROIPRO 02-1918 (UNSL) and PIP 112-2015 01-00090 (CONICET).

**References**

[1] Lin L-G, Lam Ung CO, Feng Z-L, Huang L, Hu H. (**2016**) Naturally occurring diterpenoid dimers: source, biosynthesis, chemistry and bioactivities. *Planta Medica*, ***82***, 1309-1328.

[2] Funes M, Tonn C, Kurina-Sanz M. (**2018**) *In vivo* photoinduced [4+2] dimerization of a *neo*-clerodane diterpene in *Baccharis flabellata.* ROS and RNS scavenging abilities. *Journal of Photochemistry and Photobiology B: Biology*, ***186***, 137-143.

[3] Wagner H, Seitz R, Lotter H. (**1978**) New furanoid ent-clerodanes from *Baccharis tricuneata*. *Journal of Organic Chemistry*, ***43***, 3339-3345.

[4] Ceñal JP, Giordano O, Rossomando PC, Tonn CE. (**1997**) Neoclerodane diterpenes from *Baccharis crispa*. *Journal of Natural Products*, ***60***, 490-492.

[5] Juan Hikawczuk V, López Verrilli M, Borkowski E, Sosa M, Giordano O, Saad J, Tonn C. (**2006**) Antifeedant activity of *neo*-clerodane diterpenes from *Baccharis flabellata* Hook Arn var. *flabellata* toward *Tribolium castaneum* Herbst: structure-activity relationships. *Natural Products Research*, ***20***, 813-819.

[6] Rodriguez MV, Sortino MA, Ivancovich JJ, Pellegrino JM, Favier LS, Raimondi MP, Gattuso MA, Zacchino SA. (**2013**) Detection of synergistic combinations of *Baccharis* extracts with terbinafine against *Trichophyton rubrum* with high throughput screening synergy assay (HTSS) followed by 3D graphs. Behavior of some of their components. *Phytomedicine*, ***20***, 1230-1239.

[7] Weitzman I, Summerbell R. (**1995**) The dermatophytes. *Clinical Microbiology Reviews*, ***8***, 240-259.

[8] Cribier BJ, Bakshi R. (**2004**) Terbinafine in the treatment of onychomycosis: a review of its efficacy in high-risk populations and in patients with nondermatophyte infections. *British Journal of Dermatology*, ***150***, 414-420.

[9] Wagner H, Ulrich-Merzenich G. (**2009**) Synergy research: approaching a new generation of phytopharmaceuticals. *Phytomedicine*, ***16***, 97-110.

[10] Vitale R, Afeltra J, Dannaoui E. (**2005**) Antifungal combinations. In *Antifungal Agents.* Erika J, Ernst P, Rogers D (Eds). Humana Press, Totowa, New Jersey, 143-152.

[11] Martinez Irujo JJ, Villahnosu ML, Alberdi E, Santiago E. (**1996**) A checkerboard method to evaluate interactions between drugs. *Biochemical Pharmacology*, ***51***, 635-644.

[12] Dreßler V, Müller G, Sühnel J. (**1999**) *CombiTool*-A new computer program for analyzing combination experiments with biologically active agents. *Computers and Biomedical Research*, ***32***, 145-160

[13] Iten F, Saller R, Abel G, Reichling J. (**2009**) Additive antimicrobial effects of the active components of the essential oil of *Thymus vulgaris*-chemotype carvacrol. *Planta Medica*, ***75***, 1231-1236.

[14] Clinical and Laboratory Standards Institute (CLSI). (**2008**) *Reference method for broth dilution antifungal susceptibility testing for filamentous fungi M-38 A2, vol. 28, No. 16., second ed.* Wayne PA, USA, 1-35.

[15] Rühl M, Kües U. (**2009**) Automated image analysis to observe pellet morphology in liquid cultures of filamentous fungi such as the basidiomycete *Coprinopsis cinerea*. *Current Trends in Biotechnology and Pharmacy*, ***3***, 241-253.

[16] Chou T-Ch. (**2010**) Drug combinations studies and their synergy quantification using the Chou-Talalay method. *Cancer Research*, ***70***, 440-446.

**Fungus-Growing Ant's Microbial Interaction of *Streptomyces* sp. and *Escovopsis* sp. through Molecular Networking and MALDI Imaging**
Cristopher A. Boya P., Christian Martin H., Hermógenes Fernández-Marín and Marcelino Gutiérrez **63**

**Morphological and Phytochemical Characterization of *Piper mosenii***
Tailyn Zermiani, Matheus C. Santos, Fabiane M. Lobato, Vinicius B. Blödorn, Fernanda S. M. Andrade, Letícia C. Lacava, Thamiris Y. Inoue, Renê A. Ferreira, Elsie F. Guimarães, Marina S. Machado, Ruth M. Lucinda-Silva and Ângela Malheiros **67**

**Bioactivity Profiling of Plant Biodiversity of Panama by High Throughput Screening**
Anuradha Roy, Peter McDonald, Barbara N. Timmermann, Mahabir Gupta and Rathnam Chaguturu **71**

**Composition of Essential Oil from *Piper jacquemontianum* from Eight Provenances of Guatemala**
Armando Cáceres, Sully M. Cruz, José V. Martínez-Arevalo, Amelia T. Henriques and Miriam A. Apel **75**

**Essential Oil of *Piper oradendron* from the Pacific Slope of Guatemala**
José V. Martínez-Arévalo, Sully M. Cruz, Miriam A. Apel, Amélia T. Henriques and Armando Cáceres **79**

**Effects of Essential Oils from Two Species of Piperaceae on Parasitized and Unparasitized Eggs of *Oebalus insularis* (Heteroptera: Pentatomidae) by *Telenomus podisi* (Hymenoptera: Platygastridae)**
Bruno Zachrisson, Ana Santana and Mahabir Gupta **83**

## *Accounts/Reviews*

**Alkaloids of the Cactaceae — The Classics**
Bruce K. Cassels **85**

**Essential Oils as Chemical Reagents in Heterocyclic Synthesis**
Vladimir V. Kouznetsov **91**

## *Original Paper*

**New Abietane-type Diterpenoids from the Bark of *Cryptomeria japonica***
Chi-I Chang, Jih-Jung Cheng, Chin Hsu, Cheng-Chi Chen, Wei-Yi Cheng, Sheng-Yang Wang, Ching-Kuo Lee, Ming-Jen Cheng and Yueh-Hsiung Kuo **97**

**Cladieunicellin T, a New Eunicellin-based Diterpenoid Produced by the Octocoral *Cladiella* sp.**
Zhi-Jun Zhang, Bo-Rong Peng, Chiung-Chih Hu, Nai-Cheng Lin, Jia-Wen Yao, Mei-Chin Lu, Zhi-Hong Wen, Yang-Chang Wu and Ping-Jyun Sung **101**

**Chemical Constituents from Stems of *Pileostegia viburnoides***
Xiao-Jun Li, Kwan-Woo Kim, Qin-Peng Zou, Zu-Zhen Liu, Hyun-Cheol Oh, Youn-Chul Kim and Xiang-Qian Liu **103**

**Nor-kurarinone Characteristic of Chinese *Sophora flavescens***
Ryuichiro Suzuki, Utsumi Takahiro, Risa Takao and Yoshiaki Shirataki **107**

**A New Coumarin from the Roots of *Heracleum dissectum***
Changlong Zhang, Yang Gao, Yajie Peng, Xiaoqing Zhang and Hailong Zhang **111**

**A New Tetrahydrofuran Lignan from *Premna serratifolia* Wood**
So-Yeun Woo, Chin Piow Wong, Nwet Nwet Win, Shotaro Hoshino, Prema, Hla Ngwe, Ikuro Abe and Hiroyuki Morita **113**

**Screening of Insecticidal Activity of Podophyllotoxin Analogues against *Athetis dissimilis***
Zhiping Che, Yuee Tian, Jinming Yang, Shengming Liu, Jia Jiang, Mei Hu and Genqiang Chen **117**

**Synthesis, Structure and Antimicrobial Activity of Novel Metabolites from a Marine Actinomycete in Vietnam's East Sea**
Duc-Tuan Cao, Thuy-Linh Nguyen, Van-Hieu Tran, Huong Doan-Thi-Mai, Quyen Vu-Thi, Mai-Anh Nguyen, Hong-Minh Le-Thi, Van-Minh Chau and Van-Cuong Pham **121**

**Arugosins O-Q, New Fungal Metabolites from the Fungus *Xylariaceae* sp. Isolated from Leaves of *Lansium domesticum* (Meliaceae)**
Rudiyansyah, Andi Hairil Alimuddin, Masriani, Rini Muharini, Zhen Liu, Wenhan Lin, Rudolf Hartmann and Peter Proksch **125**

**Chemical Constituents from the Fungus *Antrodia cinnamomea***
Ming-Der Wu, Ming-Jen Cheng, Yen-Lin Chen, Hsun-Hsuo-Chang, Yueh-Hsiung Kuo, Chih-Chuan Lin and Ho-Cheng Wu **129**

**A Concise and Stereoselective Total Synthesis of Paecilomycin E**
A. Srinivas Reddy, Gundamalla Bhavani, Sandhya Jonnala, Rajashaker Bantu and B. V. Subba Reddy **131**

**First Stereoselective Total Synthesis of (3*S*,7*R*)-De-*O*-methylbotryosphaeriodiplodin**
Jhillu S. Yadav, Chitteti Divya Vani, Mule Chowdeswari, K. Ananthalakshmi, N. Bhasker and Basi V. Subba Reddy **135**

**Bacilohydrin A, a New Cytotoxic Cyclic Lipopeptide of Surfactins Class Produced by *Bacillus* sp. SY27F from the Indian Ocean Hydrothermal Vent**
Hong Zhou, Yu He, Yongqi Tian, Bailin Cong and Huanghao Yang **141**

**Anti-protozoal Activity of Conifer Green Needle Complex Against *Trichomonas vaginalis***
Lidia B. Kulyashova, Natalia Roschina, Tamara V. Nikitina and Vagif S. Soultanov **147**

**Commercial Essential Oil Combinations against Topical Fungal Pathogens**
Ané Orchard, Sandy F. van Vuuren and Alvaro M. Viljoen **151**

# Natural Product Communications
# 2019
Volume 14, Number 1

## Contents

***Editorial Message*** *i*

***Editorial***
*Pawan K. Agrawal* *iii*

***Preface***
*K.S. Jagannatha Rao, Matthias Hamburger, Rachel Mata, Susana Zacchino* *v*

***Original Paper*** ***Page***

**Synergism between Terbinafine and a *Neo*-clerodane Dimer or a Monomer Isolated from *Baccharis flabellata* against *Trichophyton rubrum***
María Victoria Rodriguez, Estefanía Butassi, Matías Funes and Susana A. Zacchino **1**

***In Vivo* and *In Vitro* α-Glucosidase Inhibitory Activity of Perfoliatin A from *Melampodium perfoliatum***
Laura Flores-Bocanegra, Rafael Torres-Colín, Martin González-Andrade, José S. Calderón and Rachel Mata **5**

**Triterpenoidal and Phenolic Compounds Isolated from the Aerial Parts of *Helicteres hirsuta* and their Cytotoxicity on Several Cancer Cell Lines**
Triet Thanh Nguyen, Nadine Kretschmer, Eva-Maria Pferschy-Wenzig, Olaf Kunert and Rudolf Bauer **7**

**A Selective Ion HPLC-APCI-MS Method for the Quantification of Pentacyclic Triterpenes in an Anxiolytic Botanical Dietary Supplement for the Animal Health Market**
Rui Liu, Ana-Francis Carballo-Arce, Ranpreet Singh, Ammar Saleem, Marco Rocha, Martha Mullally, Marco Otarola-Rojas, Luis Poveda Alvarrez, Pablo Sanchez-Vindas, Mario Garcia, John Baker, Zul Merali, Jose-Antonio Guerrero-Analco, Tony Durst, Cory Harris and John Arnason **11**

**Identification of Major α-Glucosidase Inhibitors from Stem Bark of Panamanian Mangrove Plant *Pelliciera rhizophorae***
Lilia Cherigo and Sergio Martínez-Luis **15**

**Triterpenoid Saponins from the Roots of *Glycyrrhiza glabra***
Qingyao Shou, Ping Jiao, Mei Hong, Qi Jia, Indra Prakash, Sangphyo Hong, Bin Wang, Allison Bechman and Gil Ma **19**

**Chemical Characterization of the Hydroethanolic Extract of the Inner Stem Bark of *Dilodendron bipinnatum*. Comparative Cytotoxic Evaluation and Anti-inflammatory Potential of a Simple Mixture of its Isolates 3-*O*-β-Glucopyranosyl-β-sitosterol and 3-*O*-β-Glucopyranosyl-stigmasterol**
Karoline Costa Lima, Domingos Tabajara de Oliveira Martins, Antonio Macho, Ruberlei Godinho de Oliveira, Eduarda Pavan, Lorena Suelen Ribeiro Martelli, Leila Beatriz Silva Pacheco, Virgínia Claudia da Silva, Tereza Auxiliadora Nascimento Ribeiro, Mário Geraldo de Carvalho and Paulo Teixeira de Sousa Jr **23**

**Biotransformation to Produce the Anticancer Compound Colchicoside Using Cell Suspension Cultures of *Astragalus vesicarius* Plant Species**
Yancho Zarev, Pavlinka Popova, Kenn Foubert, Sandra Apers, Arnold Vlietinck, Luc Pieters and Iliana Ionkova **27**

**Antiparasitic Compounds from the Panamanian Marine Bacterium *Pseudomonas aeruginosa***
Sergio Martínez-Luis, Lilia Cherigo, Carmenza Spadafora and Marcelino Gutiérrez **31**

***In vitro* Antimalarial Evaluations and Cytotoxicity Investigations of *Carica papaya* Leaves and Carpaine**
Woon-Chien Teng, Wilson Chan, Rossarin Suwanarusk, Alice Ong, Han-Kiat Ho, Bruce Russell, Laurent Rénia and Hwee-Ling Koh **33**

**Chemical Composition and Antimycoplasmic Activity of *Eugenia mattosii* Leaves, Stems and Isolated Compounds**
Giovana Vechi, Adrielli Tenfen, Ariela Maína Boeder, Lorena Hernandez-Gómez, Caio Maurício Mendes de Córdova, Franco Delle Monache and Valdir Cechinel Filho **37**

**HPLC-Based Activity Profiling for $GABA_A$ Receptor Modulators in *Murraya exotica***
Nova Syafni, Fahimeh Moradi-Afrapoli, Ombeline Danton, Anke Wilhelm, Marco Stadler, Steffen Hering, Olivier Potterat and Matthias Hamburger **41**

**Extraction Optimization of 5,7-Dihydroxy-6,8,4′-trimethoxyflavonol, a Bioactive Flavonoid from *Rubus rosifolius* (Rosaceae) Leaves**
Janieire Lorraine da Rocha Pittarello, Marcel Petreanu, Valdir Cechinel Filho, Clóvis Antonio Rodrigues, Luiz Carlos Klein-Júnior and Rivaldo Niero **47**

**Constituents of *Talisia nervosa* with Potential Utility against Metabolic Syndrome**
Yelkaira Vásquez, Jianping Zhao, Shabana I. Khan, Mahabir P. Gupta and Ikhlas A. Khan **51**

**Antiparasitic Metabolites from *Hyptis brevipes*, a Tacana Medicinal Plant**
Ivan Limachi, Claudia Condo, Camila Palma, Nelida Nina, Efrain Salamanca, Juan C. Ticona, Enrique Udaeta, Ninoska Flores, Alcides Serato, Natalio Marupa, Benigno Chao, Gladys Ibaguari, Constantino Nay, Soffie Manner, Olov Sterner and Alberto Giménez **55**

**Quantification of *Sambucus nigra* (Adoxaceae) Markers Related to Tincture Stability**
Letícia D. Testoni, Angelita B. de Souza, Clarissa de M. A. Krueger, Nara L. M. Quintão, Angelica G. Couto and Tania M. B. Bresolin **59**

*Continued inside backcover*